Research Article | Vol. 25, No. 5 | 6 Mar 2017 | OPTICS EXPRESS 5710

Optics EXPRESS

Polarization controlled directional propagation of Bloch surface wave

TATIANA KOVALEVICH,[1,*] PHILIPPE BOYER,[1] MIGUEL SUAREZ,[1] ROLAND SALUT,[1] MYUN-SIK KIM,[2] HANS PETER HERZIG,[2] MARIA-PILAR BERNAL,[1] AND THIERRY GROSJEAN[1]

[1]*Département d'Optique P.M. Duffieux, Institut FEMTO-ST, UMR 6174 CNRS, Université Bourgogne Franche-Comté, 15B Avenue des Montboucons, 25030 Besançon Cedex, France*
[2]*Optics & Photonics Technology Laboratory, Ecole Polytechnique Fédérale de Lausanne (EPFL), Rue de la Maladière 71b, Neuchâtel, CH-2000, Switzerland*
[*]*tatiana.kovalevich@femto-st.fr*

Abstract: Bloch surface waves (BSWs) are recently developing alternative to surface plasmon polaritons (SPPs). Due to dramatically enhanced propagation distance and strong field confinement these surface states can be successfully used in on-chip all-optical integrated devices of increased complexity. In this work we propose a highly miniaturized grating based BSW coupler which is gathering launching and directional switching functionalities in a single element. This device allows to control with polarization the propagation direction of Bloch surface waves at subwavelength scale, thus impacting a large panel of domains such as optical circuitry, function design, quantum optics, etc.

OCIS codes: (050.2770) Gratings; (050.5298) Photonic crystals; (230.5440) Polarization-selective devices; (240.6690) Surface waves.

References and links

1. P. Yeh, A. Yariv, L. Sun and C.S. Hong, "Electromagnetic propagation in periodic stratified media. I. General theory," J. Opt. Soc. Am. **67**(4), 423–438 (1977).
2. J. Homola, "Surface plasmon resonance sensors for detection of chemical and biological species," Chem. Rev. **108**(2), 462–493 (2008).
3. M. Kuttge, E. J. R. Vesseur, J. Verhoeven, H. J. Lezec, H. A. Atwater and A. Polman, "Loss mechanisms of surface plasmon polaritons on gold probed by cathodoluminescence imaging spectroscopy," Appl. Phys. Lett. **93**(11), 113110 (2008).
4. V. N. Konopsky and E. V. Alieva, "Photonic crystal surface waves for optical biosensors," Anal. Chem. **79**(12), 4729–4735 (2007).
5. R. Dubey, E. Barakat, M. Häyrinen, M. Roussey, S. Honkanen, M. Kuittinen and H. P. Herzig, "Experimental investigation of the propagation properties of Bloch surface waves on dielectric multilayer platform," JEOS:RP **13**(1), 5 (2017).
6. J. C. Weeber, J. R. Krenn, A. Dereux, B. Lamprecht, Y. Lacroute and J. P. Goudonnet, "Near-field observation of surface plasmon polariton propagation on thin metal stripes," Phys. Rev. B **64**(4), 045411 (2001).
7. V. N. Konopsky, "Plasmon-polariton waves in nanofilms on one-dimensional photonic crystal surfaces," New J. Phys. **12**(9), 093006 (2010).
8. F. Michelotti, B. Sciacca, L. Dominici, M. Quaglio, E. Descrovi, F. Giorgis and F. Geobaldo, "Fast optical vapour sensing by Bloch surface waves on porous silicon membranes," Phys. Chem. Chem. Phys. **12**(2), 502–506 (2010).
9. A. Sinibaldi, A. Fieramosca, R. Rizzo, A. Anopchenko, N. Danz, P. Munzert, C. Magistris, C. Barolo and F. Michelotti, "Combining label-free and fluorescence operation of Bloch surface wave optical sensors," Opt. Lett. **39**(10), 2947–2950 (2014).
10. L. Yu, B. Barakat, T. Sfez, L. Hvozdara, J. Di Francesco and H. P. Herzig, "Manipulating Bloch surface waves in 2D: a platform concept-based flat lens," LIGHT-SCI APPL **3**(1), 124 (2014).
11. E. Descrovi, T. Sfez, M. Quaglio, D. Brunazzo, L. Dominici, F. Michelotti, H. P. Herzig, O. Martin and F. Giorgis, "Guided Bloch surface waves on ultrathin polymeric ridges," Nano Lett. **10**(6), 2087–2091 (2010).
12. L. Yu, "Near-field imaging: investigations on Bloch surface wave based 2D optics and the development of polarization-retrieved characterization," Doctoral dissertation, Ecole Polytechnique Fédérale de Lausanne (2013).
13. X. Wu, E. Barakat, L. Yu, L. Sun, J. Wang, Q. Tan and H. P. Herzig, "Phase-sensitive near field Investigation of Bloch surface wave propagation in curved waveguides," JEOS:RP **9**, 14049 (2014).
14. R. Dubey, B. Vosoughi Lahijani, E. Barakat, M. Häyrinen, M. Roussey, M. Kuittinen and H. P. Herzig, "Near-field characterization of a Bloch-surface-wave-based 2D disk resonator," Opt. Lett. **41**(21), 4867–4870 (2016).

#283314 https://doi.org/10.1364/OE.25.005710
Journal © 2017 Received 22 Dec 2016; revised 16 Feb 2017; accepted 17 Feb 2017; published 2 Mar 2017

Optics EXPRESS

15. T. Kovalevich, A. Ndao, M. Suarez, M. Häyrinen, M. Roussey, M. Kuittinen, T. Grosjean and M. P. Bernal, "Tunable Bloch surface waves in anisotropic photonic crystals based on lithium niobate thin films," Opt. Lett. **41**(23), 5616–5619 (2016).
16. S. T. Koev, A. Agrawal, H. J. Lezec and V. A. Aksyuk, "An efficient large-area grating coupler for surface plasmon polaritons," Plasmonics **7**(2), 269–277 (2012).
17. D. Taillaert, H. Chong, P. I. Borel, L. H. Frandsen, R. M. De La Rue and R. Baets, "A compact two-dimensional grating coupler used as a polarization splitter," IEEE Photonics Technol. Lett. **15**(9), 1249–1251 (2003).
18. M. Scaravilli, G. Castaldi, A. Cusano and V. Galdi, "Grating-coupling-based excitation of Bloch surface waves for lab-on-fiber optrodes," Opt. Express **24**(24), 27771–27784 (2016).
19. X. B. Kang, L. J. Liu, H. Lu, H. D. Li, Z. G. Wang, "Guided Bloch surface wave resonance for biosensor designs," J. Opt. Soc. Am. A **33**(5), 997–1003 (2016).
20. W. Bogaerts, D. Taillaert, P. Dumon, D. Van Thourhout, R. Baets and E. Pluk, "A polarization-diversity wavelength duplexer circuit in silicon-on-insulator photonic wires," Opt. Express **15**(4), 1567–1578 (2007).
21. T. Barwicz, M. R. Watts, M. A. Popović, P. T. Rakich, L. Socci, F. X. Kärtner, E. P. Ippen and H. I. Smith, "Polarization-transparent microphotonic devices in the strong confinement limit," Nat. Photonics **1**(1), 57–60 (2007).

Bloch surface waves (BSWs) are electromagnetic surface states which can be excited at the interface between periodic dielectric multilayer and a surrounding medium [1]. These waves represent a very attractive alternative to surface plasmon polaritons (SPPs), which are nowadays pivotal in a large variety of applications ranging from optical circuitry to biological sensors [2]. However, SPPs undergo important limitations due to the ohmic losses of metal such as modest propagation length and heat dissipation [3]. Being an evanescent surface waves which are produced at the free end surface of a dielectric multilayer stack [4], BSWs show dramatically enhanced propagation length up to the millimiter range [5] (a few tens of micrometers for SPPs [6]) and provide new optical opportunities such as the possibility to obtain TE or TM-polarized surface waves (SPPs are limited to TM polarization) [7]. Owing to these new properties, BSWs have found numerous applications in vapor sensing [8], biosensing [4], fluorescence detection and imaging [9], and integrated optics [10,11].

A new generation of optoelectronic and biomedical technologies is expected to emerge from the development of on-chip BSW-based integrated systems. A large panel of dielectric micro and nano-elements, such as 2D-lens [10], 2D prism and grating [12], ridge waveguides [11,13], ring resonators [14], is nowadays available for controlling the propagation of BSWs, which opens the perspective of the engineering of various optical circuits. These micro-sized 2D optical components, patterned at the free end surface of the one dimensional photonic crystal (1DPhC), tailor the BSW propagation direction by locally patterning the effective refractive indices. Reaching dynamical tunability with this technological approach would require either real - time modification of the component shapes or their refractive indices, which seem to be challenging.

BSW coupling is also a crucial step in the development of dielectric surface optical functions. Directional coupling of an incident beam to a BSW can be achieved using a bulky prism coupler in the Kretschmann configuration [15] or more rarely by using Otto architecture [8]. Such techniques lead to BSW launching in a straightforward way but it suffers from low compactness and tuning the BSW propagation direction requires the rotation of both the prism and the input laser beam, which remains hard to implement. Tuning the propagation direction of optical surface waves in a ultra-compact and versatile architecture would greatly extend the level of manipulation of BSW but it remains a real challenge. Grating-based couplers offer the opportunity to launch optical guided modes and tune their propagation direction with incident polarization and in micrometer scale architectures. Such kind of couplers are routinely produced for the excitation of SPP [16] and waveguide mode [17] but they have been hardly investigated for launching BSWs [18,19].

In this work, we demonstrate a double cross grating as a BSW coupler capable of switching the propagation direction of the excited dielectric surface wave under control with incident

Optics EXPRESS

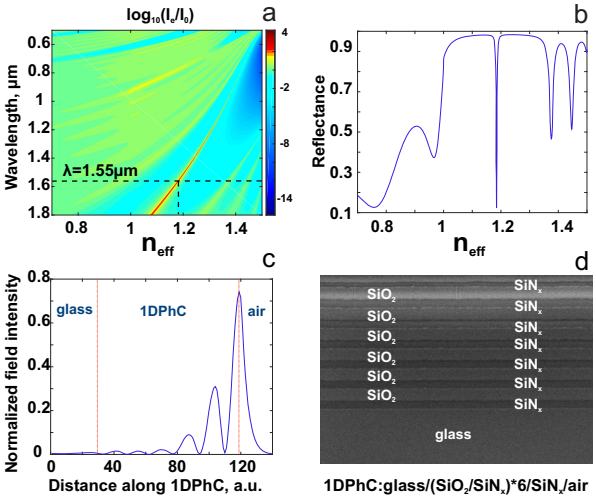

Fig. 1. (a) Band gap diagram of the 1DPhC; (b) Calculated reflectance at 1550 nm wavelength; (c) Field profile in the 1DPhC for the BSW at 1550 nm wavelength; (d) FIB-SEM image of 1DPhC.

polarization. The resulting coupler is ultra-compact and provides degrees of freedom in the control of BSWs by bringing polarization controlled tunability of BSW propagation direction. The flow of light at subwavelength scale on dielectric surfaces becomes controllable with the incident polarization, thus strongly impacting the design of future generation of all-dielectric nano-optical surface devices.

The 1DPhC is designed to support a TE polarized BSW at the wavelength of 1550 nm (TM or TM-like modes do not exist). The platform is composed of dielectric layers with alternating refractive indices. Six pairs of silicon dioxide and silicon nitride, with refractive indices of 1.45 and 1.79 at $\lambda = 1550$ nm, respectively, were deposited on a glass wafer ($n_g = 1.501$). The thicknesses of the layers are 492 nm and 263 nm, respectively. An 80-nm-thick layer of silicon nitride is deposited on top of the 1DPhC.

We modeled the structure as for the prism coupler using an impedance approach [7]. The dispersion curve for this 1DPhC is shown in the Fig. 1(a), where I_0 is a field intensity of the incident light and I_e is a field intensity at 1DPhC top layer and air interface. Indeed, for the wavelength of 1550 nm the BSW occurs inside the band gap when the effective refractive index of BSW (n_{BSW}) equals to 1.186. The reflectance minimum shown in the Fig. 1(b) indicates that the designed multilayer is optimized for these parameters. Typical field profile within the 1DPhC for the BSW mode is obtained and shown at Fig. 1(c), where the evanescent decay at the 1DPhC/air interface can be clearly observed.

The platform is fabricated using plasma-enhanced chemical vapor deposition. In order to verify the quality and the thickness of the deposited layers and to minimize the damage of the sample, Focused ion beam - Scanning Electron Microscopy (FIB-SEM) measurements were done [Fig. 1(d)]. FIB was used in order to open up a small area for sample characterization.

For the grating couplers, the strong coupling occurs when the wavevector matching condition is fulfilled as below:

$$k_{||} = k_{BSW} \pm mK, \tag{1}$$

where $k_{||}$ is $k \cdot sin\theta$ with k bring the incident wavevector and θ the incident angle, k_{BSW} is the BSW wavevector, K is the grating vector defined as $K = 2\pi/\Lambda$, when Λ is the period of

Optics EXPRESS

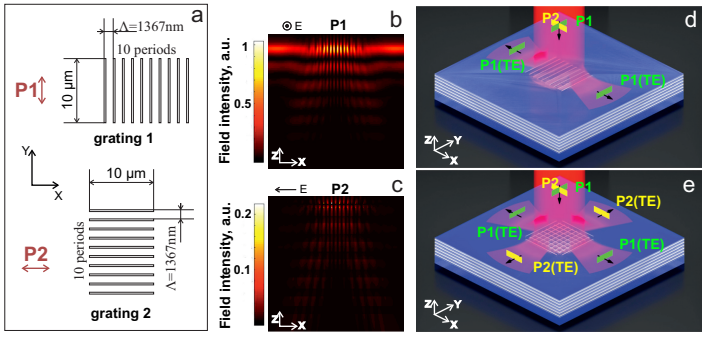

Fig. 2. (a) Polarization with respect to gratings; (b) Field profile in 1DPhC for the grating illuminated by TE polarized light; (c) Field profile in 1DPhC for the grating illuminated by TM polarized light; (d) Illustration of the BSW coupling at the single grating; (e) Illustration of the BSW coupling at the inter-crossed grating.

grating, and m is the diffraction order number. We consider a grating, whose first diffraction order couples into the surface wave at a normal incidence, i.e., $\theta = 0$. Therefore, the condition $k_{BSW} = K$ leads to the grating period Λ equal to λ_{BSW} , obtained by $\lambda/n_{BSW} = 1.306\ \mu m$. We begin with this analytical result to optimize the grating design in Rigorous Coupled Waves Analysis (RCWA).

Let us define polarizations P1 - when the electric field vector is parallel to the grating 1 with periodicity along X direction (TE polarization with respect to grating 1), and P2 - when the electric field vector is parallel to the grating 2 with periodicity along Y direction (TE polarization with respect to grating 2) [Fig. 2(a)]. For the analytically calculated value of the period for a single grating 1 coupler and randomly chosen parameters of grove depth and width FDTD simulations were performed for both P1 and P2 polarized incident light (Fig. 2(b) and Fig. 2(c) respectively). Here it can be seen that for the single grating 1 the BSW coupling occurs only for the polarization P1 [Fig. 2(d)]. However, a 2D grating can couple both incident polarizations to TE polarized BSWs of their own direction [20,21]. This way the 2D grating coupler acts as a polarization dependent beamsplitter and, in a general case with random incident light polarization, it allows the propagation of BSWs in orthogonal directions [Fig. 2(e)].

In order to take into account the influence of the groove size in the grating on BSW coupling additional calculations with RCWA method were performed. For our experimental conditions, where the light comes orthogonally to the sample surface, some part of light is transmitted, some is reflected and some is absorbed [Fig. 3(a)]. Here the absorption part is responsible for the BSW coupling. Therefore such parameters of the grating as a period (Λ), depth (h) and width(a) of the grooves were optimized according to the maximum of absorption: $\Lambda = 1367$ nm, $h = 712$ nm and $a = 136$nm. Field profile within the photonic crystal for the optimized parameters is shown at the Fig. 3(b). Here we can see that numerically achieved value for the grating period is slightly different from the analytically predicted one.

The numerically optimized grating was manufactured by FIB milling. SEM image of the grating cross-section is shown at the Fig. 3(c). For this image the thin layer of Pt was deposited in-situ on the top of 1DPhC for high resolution of the cross-section. 10 grooves of 10 μm in (X) and (Y) directions were made [Fig. 3(d)]. SEM images of the grating in this work are tilted for better visualization.

The experimental setup for sample characterization is shown at the Fig. 4(a). The light was focused through the objective (NA=0.65) at the sample surface. By adjusting the incident beam diameter with respect to the objective's front lens diameter we obtain the spot which can cover the grating. Polarization was rotated by a half-wave plate. The signal was detected in reflection

Optics EXPRESS

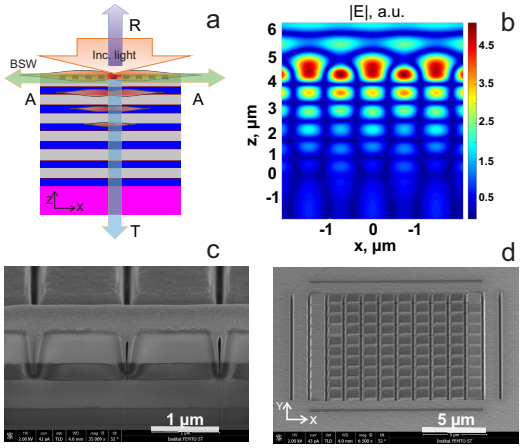

Fig. 3. (a) Schema of light propagation in 1DPhC for RCWA; (b) Field profile in 1DPhC for optimized grating parameters (RCWA simulations); (c) SEM image of the grating cross-section; (d) SEM image of the manufactured grating.

mode by the infrared camera (Xenics XEVA-2232).

In order to detect the presence of the BSW additional groves (200 nm width, 400 nm depth) were milled by FIB at the distance of 30 μm from the grating [Fig. 4(b)]. By illuminating the cross-grating by polarization P1 [Fig. 2(d)] the grating 1 with periodicity along the X-axis [Fig.4(b)] works as a BSW coupler, BSW propagates along the surface and partially decouples at the ridge A [Fig. 4(c)]. By illuminating the cross-grating by polarization P2 [Fig. 2(d)] the grating 2 with periodicity along the Y-axis [Fig. 4(b)] works as a BSW coupler, BSW partially decouples at the ridge B [Fig. 4(d)]. Decoupled light is collected by a camera. Images of the cross-sections for both gratings are shown at Fig. 4(e).

Figures 4(c) and 4(d) show the limit positions when we switch the polarization of the incident beam from the state where only P1 or P2 is present. The incident beam covers the grating, light couples into the BSW, propagates along the sample surface and partially decouples on the grove, what can be seen as a bright line at the side from the incident beam spot. If both components of polarization are present in the incident beam it is possible to control the amount of energy propagating in each direction [Fig. 5(a)].

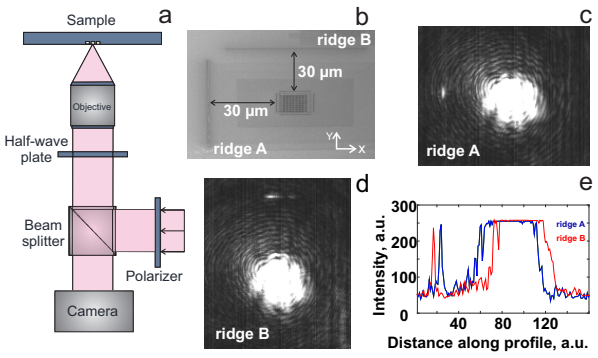

Fig. 4. (a) Experimental setup for sample characterization; (b) SEM image of the sample; (c) Camera image of the horizontally coupled BSW; (d) Camera image of the vertically coupled BSW; (e) Cross-sections for vertically and horizontally coupled BSWs.

Optics EXPRESS

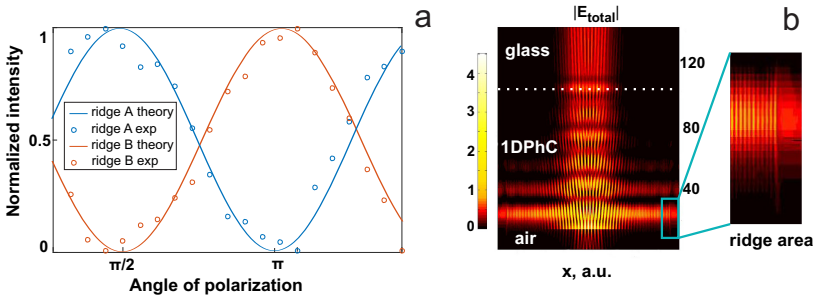

Fig. 5. (a) Intensity of the the decoupled light at the ridge A and B depending on polarization of incident beam; (b) Field profile of 1DPhC with the optimized grating and diffusers made by FDTD simulations.

The BSW is not totally decoupled at the ridge and keep propagating for the distance more than 30 μm, what can be seen from the FDTD simulations [Fig. 5(b)]. To estimate coupling efficiency of the device numerical simulations were performed. The coupling was calculated as a ratio of the flux of the pointing vector over the surfaces of the coupling area and incident light area. According to these calculations about 18% of energy is coupled into BSW with this grating configuration.

In current experimental configuration, it is hard to measure the coupling efficiency directly. Therefore, in order to check the correlation between numerical results and experimental data, we compare the amount of decoupled light from experiment and simulation by normalizing them with respect to the reflected light. For the proper quantitative analysis, we use non-saturated image of reflected and decoupled light. In order to estimate experimentally achieved decoupling at the ridge, we calculate the ratio of intensities over the surface of the decoupling area and incident beam area, which is 0.65%. The ratio between decoupled light at the ridge and reflected light from numerical simulations is 0.80%. This values are in a good agreement, therefore we can assume that coupling efficiency of the device, which used for experiments, is close to the numerically obtained one.

In summary, we have demonstrated a grating coupler on a BSW sustaining platform was designed and fabricated. Grating parameters were analytically and numerically optimized by different methods in order to obtain the best coupling conditions for given 1DPhC. The light is launched orthogonally to the multilayer. Due to a special grating configuration we demonstrate directionality of the BSW propagation depending on polarization of the incident light. The structure was experimentally realized on the surface of the 1DPhC crystal by FIB milling. Estimated coupling efficiency of the design was calculated, which is in theory reaches 18% for our case. Experimental results are in a good agreement with a theory. The investigated configuration can be successfully used as a BSW launcher in on-chip all-optical integrated systems and work as a surface wave switch or modulator.

With a grating launcher and the BSW propagation direction control with polarization of the incident light we reach a higher degree of control of Bloch surface waves. We obtain control of the propagation direction from the macro-scale down to the nano-scale. Also with the inter-crossed grating coupler we have new functionalities with simplified technologies and high degree of integration.

Funding

Collégium SMYLE (SMart SYstems for a better LifE); ANR ASTRID project “Esencyal” (ANR-13-ASTR-0019-01); LABEX ACTION (ANR-11-LABX-0001-01); The French RENATECH network and its FEMTO-ST technological facility.